

## Dephasing in a quantum dot coupled to a quantum point contact

Tomosuke Aono

*Department of Physics, Ben-Gurion University of the Negev, Beer-Sheva 84105, Israel*

(Received 30 August 2007; revised manuscript received 13 December 2007; published 21 February 2008)

We investigate a dephasing mechanism in a quantum dot capacitively coupled to a quantum point contact. We use a model which was proposed to explain the 0.7 structure in point contacts, based on the presence of a quasibound state in a point contact. The dephasing rate is examined in terms of charge fluctuations of electrons in the bound state. We address a recent experiment by Avinun-Kalish *et al.* [Phys. Rev. Lett. **92**, 156801 (2004)], where a double-peak structure appears in the suppressed conductance through the quantum dot. We show that the two conducting channels induced by the bound state are responsible for the peak structure.

DOI: [10.1103/PhysRevB.77.081303](https://doi.org/10.1103/PhysRevB.77.081303)

PACS number(s): 73.23.-b, 03.65.Yz, 72.15.Qm, 74.50.+r

Coherent transmission of electrons through a quantum dot (QD) has been investigated using an Aharonov-Bohm (AB) interferometer to understand phase coherent transport. For this purpose, controlled dephasing experiments are essential. In Refs. 3 and 4, experiments were performed using mesoscopic structures with QDs. Reference 3 measured the suppression of coherent transmission through a QD embedded in an AB ring. A quantum point contact (QPC) is capacitively coupled to a QD in the Coulomb blockade regime. Adding an electron to the QD changes the transmission probability  $T$  through the QPC by  $\Delta T$ . When the source-drain voltage  $V_{\text{QPC}}$  through the QPC is finite, there are the current fluctuations—i.e., the shot noise. The QPC then induces dephasing in the QD. The visibility of the AB interference pattern is  $1 - \alpha$ ,<sup>3,5-7</sup> with the suppression strength  $\alpha = \gamma/\Gamma$ , where  $\Gamma$  is the level width of the QD and  $\gamma$  is the dephasing rate:

$$\gamma = \frac{eV_{\text{QPC}}}{8\pi} \frac{(\Delta T)^2}{T(1-T)}. \quad (1)$$

Recently a controlled dephasing experiment was investigated for the QD in the Kondo regime.<sup>8</sup> Preceding this experiment, Silva and Levit addressed the problem using the slave-boson mean-field theory.<sup>9</sup> The conductance  $G$  of the QD is suppressed by  $\Delta G = -G(V_{\text{QPC}}=0)\alpha$  with

$$\alpha = \frac{\gamma}{T_K}, \quad (2)$$

where  $T_K$  is the Kondo temperature. Later, Kang<sup>10</sup> using the  $1/N$  expansion calculated that

$$\alpha = \frac{\gamma^2}{\gamma^2 + T_K^2}. \quad (3)$$

The experiment demonstrated several interesting features. One of them is the magnitude of  $\alpha$ . It is about 30 times larger than Eq. (2). Kang<sup>10</sup> showed that the dephasing rate can be large when the QPC is geometrically asymmetric. Another intriguing result is that  $\alpha$  shows a double-peak structure as a function of  $T$ . This result has not yet been addressed, and it is natural to associate the problem with another intriguing feature of the QPC: the 0.7 structure.<sup>11,12</sup>

In many experiments, the conductance  $G_{\text{QPC}}$  through the QPC shows an additional plateau near  $G_{\text{QPC}} = 0.7 \times 2e^2/h$  at

zero magnetic field.<sup>11-16</sup> Further experiments have been performed<sup>17-21</sup> to understand the features that cannot be explained by the conventional point contact model. In parallel, many theoretical studies have been made using different models, including an antiferromagnetic Wigner crystal,<sup>22</sup> spin split models,<sup>23-29</sup> and numerical calculations using the density functional theory.<sup>23,30-33</sup> References 31-33 demonstrated the formation of a quasibound state in the QPC, which is responsible for localized spins near the QPC. Grounded in this finding, a generalized Kondo model has been invoked to describe transport properties through the QPC.<sup>34</sup> The bound state and the Coulomb interaction in the QPC cause an additional plateau of  $G$ , which exhibits the Kondo effect. Kondo physics has been observed at low temperature and voltage bias.<sup>15</sup> In addition, recent experiments<sup>35,36</sup> measured the shot noise through the QPC as a function of magnetic field. The results indicate two conducting channels with different transmission amplitudes. Reference 37 showed that the model<sup>34</sup> is consistent with the experimental results in Refs. 35 and 36.

In this paper, we investigate a dephasing mechanism in a QD using the generalized Kondo model<sup>34</sup> in a QPC. The dephasing rate is examined in terms of charge fluctuations of the quasibound state in a QPC. The presence of the state in the QPC accounts for a dephasing mechanism which is qualitatively different from the mechanism without the bound state. The two conducting channels due to the bound state are responsible for a double-peak structure of the dephasing rate, which is observed in Ref. 8.

We consider a QD-QPC hybrid system as depicted in Fig. 1(a). The model Hamiltonian of the system consists of three parts  $H_{\text{QPC}}$ ,  $H_{\text{QD}}$ , and  $H_{\text{QPC-QD}}$  as shown below.

The model Hamiltonian of the QPC proposed in Ref. 34 is the generalized Kondo model:  $H_{\text{QPC}} = H_{\text{lead}} + H_{\text{sd}}$  with

$$H_{\text{lead}} = \sum_{k\sigma \in L,R} \epsilon_{k\sigma} \bar{c}_{k\sigma} c_{k\sigma}, \quad (4)$$

$$H_{\text{sd}} = \sum_{k,k'\sigma \in L,R} (J_{kk'}^{(1)} - J_{kk'}^{(2)}) \bar{c}_{k\sigma} c_{k'\sigma} + 2 \sum_{k,k'\sigma\sigma' \in L,R} (J_{kk'}^{(1)} + J_{kk'}^{(2)}) \bar{c}_{k\sigma} \vec{\sigma}_{\sigma\sigma'} c_{k'\sigma'} \cdot \vec{S}, \quad (5)$$

where

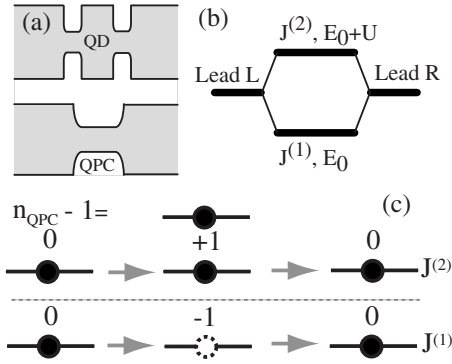


FIG. 1. (a) Schematic view of a QD coupled to a QPC. (b) The two-channel model of the QPC. It consists of two conducting channels due to Kondo coupling constants  $J^{(i)} (i=1, 2)$ , which work as an Aharonov-Bohm interferometer in the QPC. (c) The charge fluctuations due to the transmission through the  $J^{(1)}$  and  $J^{(2)}$  channels. The numbers indicate  $n_{\text{QPC}} - 1$ .

$$J_{kk'}^{(i)} = \frac{(-1)^{(i+1)}}{4} \left[ \frac{V_k^{(i)} V_{k'}^{(i)}}{\varepsilon_k - E^{(i)}} + \frac{V_k^{(i)} V_{k'}^{(i)}}{\varepsilon_{k'} - E^{(i)}} \right] \quad (6)$$

and  $\bar{c}_{k\sigma}$  creates an electron with momentum  $k$  and spin  $\sigma$  in lead  $L$  and  $R$ ;  $E^{(1)} = E_0$  and  $E^{(2)} = E_0 + U$  with the energy level of local spin state  $E_0$  and the Coulomb energy  $U$ .  $\bar{S}$  is the local spin due to the localized state. We assume  $J_{kk'}^{(i)} = J^{(i)}$ . The exponential increase of the couplings is modeled by a Fermi function  $f_{\text{FD}}(x) = 1/[1 + \exp(x)]$ , leading to the Fermi energy  $E_F$  dependence of  $J^{(i)}$ :  $J^{(i)} = \frac{(-1)^{(i+1)}(V^{(i)})^2}{E_F - E^{(i)}} f_{\text{FD}}(-E_F/\delta)$ , where  $\delta$  is a constant that characterizes the gate voltage range between the conductance plateaus in the QPC.

The Hamiltonian of the QD is the conventional Anderson model:  $H_{\text{QD}} = \sum_{k,\sigma} \sum_{\alpha=L,R} \varepsilon_k \bar{f}_{k\sigma\alpha} d_{k\sigma\alpha} + \sum_{\sigma} \varepsilon_0 \bar{d}_{\sigma} d_{\sigma} + U_d n_{\uparrow} n_{\downarrow} + V_T \sum_{k,\sigma} \sum_{\alpha=L,R} [\bar{f}_{k\sigma\alpha} d_{\sigma} + \text{H.c.}]$ , where  $\bar{d}_{\sigma}$  creates an electron in the QD with spin  $\sigma$ , while  $\bar{f}_{k\sigma\alpha}$  creates an electron with momentum  $k$  and spin  $\sigma$  in the lead  $\alpha$  attached to the QD with the tunneling matrix element  $V_T$ ;  $n_{\sigma} = \bar{d}_{\sigma} d_{\sigma}$ , and  $\varepsilon_0$  and  $U_d$  are the energy level and the Coulomb energy in the QD, respectively.

The third part of the Hamiltonian,  $H_{\text{QPC-QD}}$ , describes the interaction between the QPC and the QD. Localized electrons in the QPC interact with the electrons in the QD:

$$H_{\text{QPC-QD}} = W n_{\text{QPC}} \sum_{\sigma} n_{\sigma}, \quad (7)$$

where  $n_{\text{QPC}}$  is the number of localized electrons in the QPC and  $W$  is the coupling constant. The energy level in the QD is shifted by  $H_{\text{QPC-QD}}$ :  $\varepsilon_0 \rightarrow \varepsilon_0 + W n_{\text{QPC}}$ .

The conductance through the QPC was calculated using second-order perturbation theory:<sup>34,38</sup>  $G_{\text{QPC}} = 2e^2 T/h$  with

$$T = 4\pi^2 \rho^2 [(J^{(1)} - J^{(2)})^2 + 3(J^{(1)} + J^{(2)})^2] \quad (8)$$

and the density of states,  $\rho$ , in the leads. We have introduced a renormalized coupling constant  $J^{(2r)} = 1/[4\rho \ln(T/T_K)]$  with the Kondo temperature  $T_K = U \exp[-1/(4\rho J^{(2)})]$ , which char-

acterizes the Kondo effect in the QPC.<sup>34</sup> The right-hand side of Eq. (8) consists of three terms proportional to  $(J^{(1)})^2$ ,  $(J^{(2r)})^2$ , and  $J^{(1)} J^{(2r)}$ . This combination of the terms indicates an AB interferometer picture with the  $J^{(1)}$  and  $J^{(2)}$  channels in the QPC as depicted in Fig. 1(b). Note that the appearance of the  $J^{(1)} J^{(2)}$  term is not peculiar to the Kondo model (5). When multichannels involve electron transport, interference between them occurs.

The electron transport through the QPC induces fluctuations of  $n_{\text{QPC}}$  since Eq. (5) is an effective Hamiltonian in the presence of a localized electron and cotunneling processes via charge excitation states described by  $J^{(i)}$  in Eq. (6). If no current flows through the QPC,  $n_{\text{QPC}} = 1$ . When electrons pass through the  $J^{(1)}$  channel, virtual excitations from  $n_{\text{QPC}} = 1$  to  $n_{\text{QPC}} = 0$  are involved, while when electrons pass through the  $J^{(2)}$  channel, excitations to  $n_{\text{QPC}} = 2$  are involved. These situations are depicted in Fig. 1(c) with  $n_{\text{QPC}} - 1$ . This change in  $n_{\text{QPC}}$  shifts  $\varepsilon_0$  in the QD. In this way, the transmission of electrons through the QPC is monitored by electrons in the QD. The current fluctuations (shot noise) through the QPC lead to fluctuations in  $n_{\text{QPC}}$  and eventually in  $\varepsilon_0$ . It has been shown that the fluctuations of  $\varepsilon_0$  due to the external environment lead to dephasing in the QD, where the time evolution of  $d_{\sigma}$  shows an exponential decay due to the fluctuations.<sup>6</sup>

Transport through the ‘‘AB ring’’ in the QPC is monitored by the QD through these charge fluctuations. The terms proportional to  $(J^{(1)})^2$  and  $(J^{(2r)})^2$  give the transmission probability of the excited states with  $n_{\text{QPC}} - 1 = \mp 1$ , respectively. The  $J^{(1)} J^{(2r)}$  term, on the other hand, describes the overlap between the transmission coefficients of the excited states with  $n_{\text{QPC}} - 1 = \mp 1$ . The QD cannot monitor this overlap effectively compared to the  $(J^{(1)})^2$  and  $(J^{(2r)})^2$  terms. This is because the QD can detect  $n_{\text{QPC}} - 1$  through the Coulomb interaction (7), and accordingly the fluctuations of  $\varepsilon_0$  in the QD for this term are much smaller than the other terms. Thereby the current fluctuations of the  $(J^{(1)})^2$  and  $(J^{(2r)})^2$  terms contribute to the dephasing in the QD while those of the  $J^{(1)} J^{(2r)}$  term can be negligible.

The dephasing rate  $\gamma$  is then the sum of the dephasing rates of the two independent channels:  $(J^{(1)})^2$  and  $(J^{(2r)})^2$  terms. In each channel, we use the result of the previous theories<sup>3,5-7</sup> for a single-channel QPC model. The measured  $\Delta T$  characterizes the interaction between the QPC and QD. The total dephasing rate  $\gamma$  is, instead of Eq. (1),

$$\gamma = \frac{eV_{\text{QPC}}}{8\pi} [\gamma_0(T_1) + \gamma_0(T_2)], \quad (9)$$

with  $\gamma_0(T) = [\Delta T(T)]^2 / T(1-T)$ , where  $T_i$  is the transmission probability through the channel  $J^{(i)}$ :

$$T_{1/2} = 4\pi^2 \rho^2 [(J^{(1/2)})^2 + 3(J^{(1/2r)})^2]. \quad (10)$$

The common factor of  $\Delta T(T)$  appears for both transmission channels. This is because  $\Delta T$  is measured by adding an electron to the QD, and this affects both channels equally.

We calculate  $\gamma$  in Eq. (9) as a function of  $T$  in Eq. (8). We use a perturbative approach with

$$\bar{T} = \frac{T}{1+T} \quad (11)$$

and

$$\bar{T}_i = \frac{T_i}{1+T_i} \quad (12)$$

in place of  $T$  and  $T_i$ . This corresponds to taking into account the perturbative corrections to  $H_{\text{lead}}$  by  $H_{\text{sd}}$ . The current through the QPC is calculated in the following way. We expand the Keldysh action  $T_c \exp(-iS_{\text{sd}})$ , where  $S_{\text{sd}}$  is the action of the Kondo interaction (5) and the time order is taken along the Keldysh contour. We expand the action up to the second order in  $J^{(i)}$  and reduce it to the bilinear form with respect to conduction electron fields using Wick's theorem.<sup>39</sup> Then we have a noninteracting model without  $H_{\text{sd}}$  and with the renormalized action  $\tilde{S}_0$  for the kinetic term of conduction electrons. Then the current through the QPC is calculated with  $\tilde{S}_0$  and the current operator  $I = ie/\hbar [\sum_{k \in L, k' \in R, \sigma} (J^{(1)} - J^{(2)}) \bar{c}_{k\sigma} c_{k'\sigma} + 2 \sum_{k, \sigma \in L} (J^{(1)} + J^{(2)}) \bar{c}_{k\sigma} \vec{\sigma}_{\sigma\sigma'} c_{k'\sigma'} \cdot \vec{S}] + \text{H.c.}$  The transmission probability is then given by Eq. (11). If the renormalization of  $S_0$  is disregarded, where  $\tilde{S}_0 = S_0$  with the action  $S_0$  for Eq. (4), the transmission probability is given by Eq. (8). The origin of  $T$  in the denominator of Eq. (11) is the Kondo scattering in each lead, while  $T$  in the numerator is the scattering between two leads. Since the Kondo coupling constants are equal for both scattering processes, the same factor of  $T$  appears. In a similar way, the transmission probability  $T_i$  through the channel  $J^{(i)}$  acquires the denominator  $1+T_i$ .

We need to find the  $T$  dependence of  $\gamma_0$  from the experimental data. In Fig. 2(a), symbols indicate the two sets of the experimental data in Ref. 8. To fit these data, we use  $\gamma_0(T) = 0.9\sqrt{T/0.2} \times 10^{-5}$  when  $T < 0.2$  and  $\gamma_0(T) = 0.9 \exp[1 - (T/0.2)^{0.7}] \times 10^{-5}$  when  $T > 0.2$ . The plot is shown by the solid line in Fig. 2(a). This choice of  $\gamma_0$  reflects the fact that  $\Delta T$  is a highly asymmetric function with respect to  $T$ . The maximum of  $\Delta T$  is located at  $T=0.2$ . Other choices of  $\gamma_0$  will give qualitatively similar results.

In the experiments, the differential conductance through the QPC exhibited a zero-bias anomaly (ZBA) while no clear sign of the 0.7 structure was observed. In Ref. 15, a ZBA was observed, which confirms that it originates from the Kondo effect. The absence of a clear 0.7 structure does not contradict the Kondo effect but rather it indicates that the effect is strong.<sup>40</sup> In Fig. 2(b),  $G_{\text{QPC}}$  is plotted as a function of the Fermi energy  $E_F$  of conduction electrons with  $\rho(V^{(1)})^2/|E_0| = 0.25$ ,  $\rho(V^{(2)})^2/|E_0| = 0.025$ , and  $U/|E_0| = 1.5$ . The parameters are chosen so that the QPC does not show a clear 0.7 structure in  $G_{\text{QPC}}$ .

In Fig. 2(c),  $\gamma/(eV_{\text{QPC}}/8\pi) = \gamma_0(T_1) + \gamma_0(T_2)$  is plotted as a function of  $T$  by the thick solid line, while for comparison  $\gamma_0(T)$  for the conventional single-channel QPC model is shown by the thin solid line. A double-peak structure of  $\gamma$  appears as in the experiment, in contrast to a single-peak

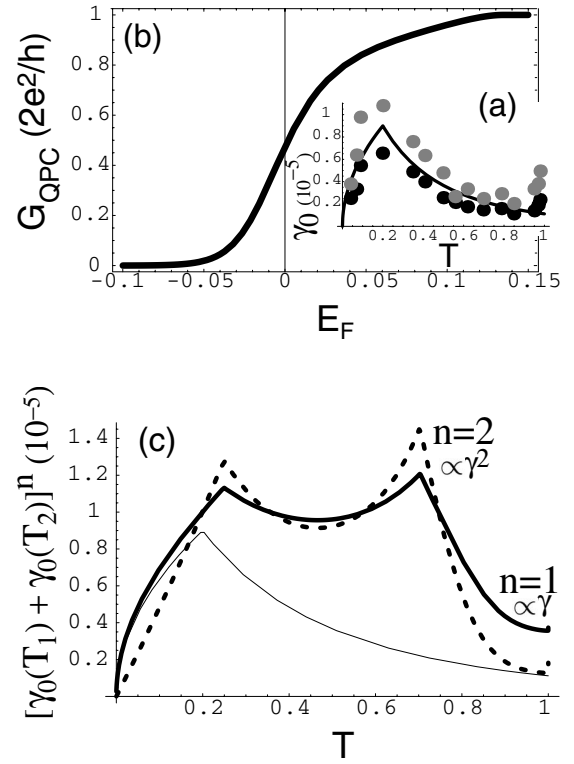


FIG. 2. (a)  $\gamma_0$  as a function of  $T$ . Symbols indicate the experimental data in Ref. 8. The solid line is the fitting curve. See also Fig. 4(c) in Ref. 8. (b)  $G_{\text{QPC}}$  as a function of the Fermi energy  $E_F$  of conduction electrons with  $\rho(V^{(1)})^2 = 0.25$ ,  $\rho(V^{(2)})^2 = 0.025$ ,  $U = 1.5$ ,  $\delta = 0.02$ , and  $k_B T = 0.001$ . The unit of energy is  $|E_0|$ . (c)  $[\gamma_0(T_1) + \gamma_0(T_2)]^n$  as a function of  $T$ . The thick solid line ( $n=1$ ) is for Eq. (9) while the thin line is for the conventional QPC model, and the dashed line ( $n=2$ ) is for Kang's result (Ref. 10).

structure. The peak positions are located at  $T \sim 0.25$  and  $T \sim 0.7$ . According to Ref. 10,  $\Delta G$  is given by Eq. (3). It is proportional to  $\gamma^2 \propto [\gamma_0(T_1) + \gamma_0(T_2)]^2$  when  $\gamma \ll T_K$ . The dashed line in Fig. 2(c) shows the result for this case. The double-peak structure becomes more pronounced.

We should mention a consequence of the asymmetric line shape of  $\Delta T$ , which questions the dephasing theory based on the conventional model of the QPC. The dephasing rate is too small when  $T \sim 0.7$  besides the absence of the extra peak. If  $\Delta T$  were symmetric,  $\gamma_0(T)$  would be symmetric around  $T = 1/2$ . The difference between the experiment and theory was then quantitative, but not qualitative. The experiment revealed an essential feature of the QPC. For the two-channel model used here, on the other hand, this asymmetry helps to show the double-peak structure.

If the 0.7 structure of  $G_{\text{QPC}}$  is observed, the second peak near  $T = 0.7$  of  $\gamma$  is sharper than the one without the 0.7 structure. This is because the conductance is changed noticeably near  $T = 0.7$ , and then the shot noise through the  $J^{(2)}$  channel changes abruptly as well.

We did not address the amplitude of  $\Delta G$ . As pointed out by Kang,<sup>10</sup> the asymmetrical structure of the QPC induces a larger dephasing rate in the experiment. In this case, the dephasing rate depends on not only  $\Delta T$ , but also on the

change of the phase shift through the QPC, which requires additional information from experiments, such as measurements in the device setup in Ref. 4.

In conclusion, we have discussed the dephasing mechanism due to charge fluctuations of a quasibound state in a quantum point contact. The bound state is responsible for there being two transmission channels. The dephasing rate is proportional to the sum of the transmission probability through these two channels. This mechanism explains the

double-peak structure of the suppression rate of the conductance, observed in a recent experiment.<sup>8</sup> The result is qualitatively different from the rate without the bound state in the QPC.

The author acknowledges fruitful discussions with Y. Meir, as well as valuable comments on the manuscript. He also thanks to M. Avinun-Kalish, Y. Dubi, A. Golub, T. Rejec, and R. S. Tasgal for discussions.

- <sup>1</sup>A. Yacoby, M. Heiblum, D. Mahalu, and H. Shtrikman, *Phys. Rev. Lett.* **74**, 4047 (1995).
- <sup>2</sup>R. Schuster, E. Buks, M. Heiblum, D. Mahalu, V. Umansky, and H. Shtrikman, *Nature (London)* **385**, 417 (1997).
- <sup>3</sup>E. Buks, R. Schuster, M. Heiblum, D. Mahalu, and V. Umansky, *Nature (London)* **391**, 871 (1998).
- <sup>4</sup>D. Sprinzak, E. Buks, M. Heiblum, and H. Shtrikman, *Phys. Rev. Lett.* **84**, 5820 (2000).
- <sup>5</sup>I. L. Aleiner, N. S. Wingreen, and Y. Meir, *Phys. Rev. Lett.* **79**, 3740 (1997).
- <sup>6</sup>Y. Levinson, *Europhys. Lett.* **39**, 299 (1997).
- <sup>7</sup>G. Hackenbroich, B. Rosenow, and H. A. Weidenmüller, *Phys. Rev. Lett.* **81**, 5896 (1998); G. Hackenbroich, *Phys. Rep.* **343**, 463 (2001).
- <sup>8</sup>M. Avinun-Kalish, M. Heiblum, A. Silva, D. Mahalu, and V. Umansky, *Phys. Rev. Lett.* **92**, 156801 (2004).
- <sup>9</sup>A. Silva and S. Levit, *Europhys. Lett.* **62**, 103 (2003).
- <sup>10</sup>K. Kang, *Phys. Rev. Lett.* **95**, 206808 (2005).
- <sup>11</sup>K. J. Thomas, J. T. Nicholls, M. Y. Simmons, M. Pepper, D. R. Mace, and D. A. Ritchie, *Phys. Rev. Lett.* **77**, 135 (1996).
- <sup>12</sup>K. J. Thomas, J. T. Nicholls, N. J. Appleyard, M. Y. Simmons, M. Pepper, D. R. Mace, W. R. Tribe, and D. A. Ritchie, *Phys. Rev. B* **58**, 4846 (1998).
- <sup>13</sup>A. Kristensen, H. Bruus, A. E. Hansen, J. B. Jensen, P. E. Lindelof, C. J. Marckmann, J. Nygård, C. B. Sørensen, F. Beuscher, A. Forchel, and M. Michel, *Phys. Rev. B* **62**, 10950 (2000).
- <sup>14</sup>D. J. Reilly, G. R. Facer, A. S. Dzurak, B. E. Kane, R. G. Clark, P. J. Stiles, J. L. O'Brien, N. E. Lumpkin, L. N. Pfeiffer, and K. W. West, *Phys. Rev. B* **63**, 121311(R) (2001).
- <sup>15</sup>S. M. Cronenwett, H. J. Lynch, D. Goldhaber-Gordon, L. P. Kouwenhoven, C. M. Marcus, K. Hirose, N. S. Wingreen, and V. Umansky, *Phys. Rev. Lett.* **88**, 226805 (2002).
- <sup>16</sup>D. J. Reilly, T. M. Buehler, J. L. O'Brien, A. R. Hamilton, A. S. Dzurak, R. G. Clark, B. E. Kane, L. N. Pfeiffer, and K. W. West, *Phys. Rev. Lett.* **89**, 246801 (2002).
- <sup>17</sup>A. C. Graham, K. J. Thomas, M. Pepper, N. R. Cooper, M. Y. Simmons, and D. A. Ritchie, *Phys. Rev. Lett.* **91**, 136404 (2003).
- <sup>18</sup>L. P. Rokhinson, L. N. Pfeiffer, and K. W. West, *Phys. Rev. Lett.* **96**, 156602 (2006).
- <sup>19</sup>T. Morimoto, M. Henmi, R. Naito, K. Tsubaki, N. Aoki, J. P. Bird, and Y. Ochiai, *Phys. Rev. Lett.* **97**, 096801 (2006).
- <sup>20</sup>R. Crook, J. Prance, K. J. Thomas, S. J. Chorley, I. Farrer, D. A. Ritchie, M. Pepper, and C. G. Smith, *Science* **312**, 1359 (2006).
- <sup>21</sup>S. Lüscher, L. S. Moore, T. Rejec, Y. Meir, H. Shtrikman, and D. Goldhaber-Gordon, *Phys. Rev. Lett.* **98**, 196805 (2007).
- <sup>22</sup>K. A. Matveev, *Phys. Rev. Lett.* **92**, 106801 (2004); *Phys. Rev. B* **70**, 245319 (2004).
- <sup>23</sup>C.-K. Wang and K.-F. Berggren, *Phys. Rev. B* **54**, R14257 (1996); **57**, 4552 (1998); A. A. Starikov, I. I. Yakimenko, and K.-F. Berggren, *ibid.* **67**, 235319 (2003).
- <sup>24</sup>D. J. Reilly, *Phys. Rev. B* **72**, 033309 (2005).
- <sup>25</sup>H. Bruus, V. V. Cheianov, and K. Flensberg, *Physica E (Amsterdam)* **10**, 97 (2001).
- <sup>26</sup>Y. Tokura and A. Khaetskii, *Physica E (Amsterdam)* **12**, 711 (2004).
- <sup>27</sup>P. S. Cornaglia and C. A. Balseiro, *Europhys. Lett.* **67**, 634 (2004).
- <sup>28</sup>A. Lassl, P. Schlagheck, and K. Richter, *Phys. Rev. B* **75**, 045346 (2007).
- <sup>29</sup>M. Kindermann, P. W. Brouwer, and A. J. Millis, *Phys. Rev. Lett.* **97**, 036809 (2006); M. Kindermann and P. W. Brouwer, *Phys. Rev. B* **74**, 125309 (2006).
- <sup>30</sup>K.-F. Berggren and I. I. Yakimenko, *Phys. Rev. B* **66**, 085323 (2002); P. Jaksch, I. I. Yakimenko, and K.-F. Berggren, *ibid.* **74**, 235320 (2006).
- <sup>31</sup>K. Hirose, Y. Meir, and N. S. Wingreen, *Phys. Rev. Lett.* **90**, 026804 (2003).
- <sup>32</sup>T. Rejec and Y. Meir, *Nature (London)* **442**, 900 (2006).
- <sup>33</sup>S. Ihnatsenka and I. V. Zozoulenko, *Phys. Rev. B* **76**, 045338 (2007).
- <sup>34</sup>Y. Meir, K. Hirose, and N. S. Wingreen, *Phys. Rev. Lett.* **89**, 196802 (2002).
- <sup>35</sup>P. Roche, J. Ségala, D. C. Glatli, J. T. Nicholls, M. Pepper, A. C. Graham, K. J. Thomas, M. Y. Simmons, and D. A. Ritchie, *Phys. Rev. Lett.* **93**, 116602 (2004).
- <sup>36</sup>L. DiCarlo, Y. Zhang, D. T. McClure, D. J. Reilly, C. M. Marcus, L. N. Pfeiffer, and K. W. West, *Phys. Rev. Lett.* **97**, 036810 (2006).
- <sup>37</sup>A. Golub, T. Aono, and Y. Meir, *Phys. Rev. Lett.* **97**, 186801 (2006).
- <sup>38</sup>J. A. Appelbaum, *Phys. Rev. Lett.* **17**, 91 (1966); *Phys. Rev.* **154**, 633 (1967).
- <sup>39</sup>It is useful to apply a unitary transformation for the conduction electrons, introducing two linear combinations of  $(c_{k\sigma} + c_{k'\sigma'})/\sqrt{2}$  and  $(c_{k\sigma} - c_{k'\sigma'})/\sqrt{2}$ , where  $k, \sigma \in L$  and  $k', \sigma' \in R$ . Then the latter is decoupled from the Kondo interaction. See also Ref. 37.
- <sup>40</sup>If a QPC model reduces to the conventional noninteracting model when the QPC does not show a clear 0.7 structure, a single peak, instead of double peaks, of  $\alpha$  may appear.